Ultrasound in Med. & Biol., Vol. 27, No. 9, pp. 1177–1183, 2001

0301-5629/01/$–see front matter

PII: S0301-5629(01)00421-5

● *Original Contribution*

REAL-TIME THREE-DIMENSIONAL INTRACARDIAC ECHOCARDIOGRAPHY

EDWARD D. LIGHT,* SALIM F. IDRISS,* PATRICK D. WOLF* and STEPHEN W. SMITH*
*Department of Biomedical Engineering, Duke University, Durham, NC, USA

(*Received* 2 *January* 2001; *in final form* 11 *June* 2001)

Abstract—Using catheter-mounted 2-D array transducers, we have obtained real-time 3-D intracardiac ultrasound (US) images. We have constructed several transducers with 64 channels inside a 12 French catheter lumen operating at 5 MHz. The transducer configuration may be side-scanning or beveled, with respect to the long axis of the catheter lumen. We have also included six electrodes to aquire simultaneous electrocardiograms. Using an open-chest sheep model, we inserted the catheter into the cardiac chambers to study the utility of *in vivo* intracardiac 3-D scanning. Images obtained include a cardiac four-chamber view, mitral valve, pulmonic valve, tricuspid valve, interatrial septum, interventricular septum and ventricular volumes. We have also imaged two electrophysiological interventional devices in the right atrium, performed an *in vitro* ablation study, and viewed the pulmonary veins *in vitro*. (E-mail: edl@duke.edu) © 2001 World Federation for Ultrasound in Medicine & Biology.

Key Words: **Two-dimensional array, Volumetric ultrasound imaging, Intracardiac echocardiography.**

INTRODUCTION

Real-time 3-D scanning for cardiac applications has received significant attention in recent years (Schmidt et al. 1999; Shiota et al. 1998; Qin et al. 2000) A 2-D array (N × N) transducer is necessary to obtain real-time volumetric images. By using a 2-D array transducer, the ultrasound (US) beam can be steered and dynamically focused in a pyramidal scan, acquiring a volume of data (Smith et al. 1991). Thus, real-time 3-D scans can be produced, and any plane within the pyramid may be displayed.

Display options include simultaneous orthogonal B-scans, acquisition and display of high speed C-scans, display of inclined planes, volumetric, angle-independent flow imaging and real-time 3-D rendering (Stetton et al. 1998). Figure 1 shows a schematic of a pyramidal scan illustrating the possible display planes.

There has also been much interest in intracardiac US using catheter-mounted transducers. By placing the catheter within the cardiac chambers, several of the challenges of transthoracic transducers can be overcome. With a total scanning depth of about 6 cm for an intracardiac transducer, higher frequency transducers can be employed to improve spatial resolution. Intracardiac circular scanning mechanical systems and side-scanning phased arrays have been developed to aid in the guidance of interventional cardiology (Bom et al. 1972; Ren et al. 1997; Seward et al. 1996). However, none of these transducers is capable of producing real-time 3-D intracardiac images. Real-time volumetric scanning could offer further improvements for guiding interventional cardiac procedures. Imaging cardiac structures in 3-D would be possible, as well as the 3-D localization of interventional catheters. The long-term monitoring of left ventricular function of patients in the intensive care unit or in the operating room might also benefit from a volumetric imaging system. By scanning the entire left ventricle, an accurate volume can be measured and monitored.

Electrocardiogram mapping electrodes are used for collecting electrophysiological data within the heart and for delivering radiofrequency (RF) ablation energy (Wharton and Ideker 1995). These devices can detect arrhythmic areas, but cannot visualize tissues. Combining the function of the ECG electrodes into our imaging device might reduce the number of catheters needed for multiple intracardiac procedures and for the visualization of ablated tissue.

In this paper, we describe initial *in vitro* and *in vivo*

Address correspondence to: Edward D. Light, Department of Biomedical Engineering, Box 90281, Duke University, Durham, NC 27708-0281 USA. E-mail: edl@duke.edu

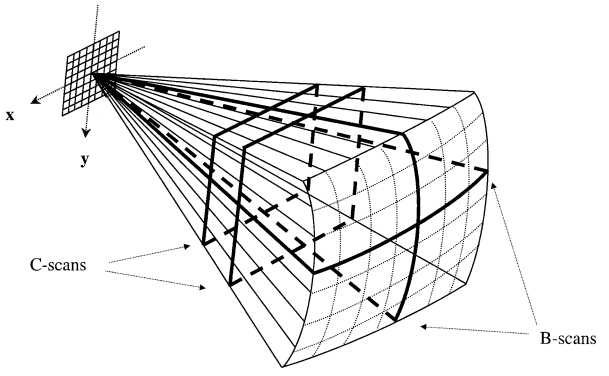

Fig. 1. Schematic of pyramidal scan volume from a 2-D array transducer. The bold lines indicate possible display planes. By integrating and spatially filtering between the two C-scans, a 3-D rendered image can be generated and displayed in real-time.

results using 3-D intracardiac echocardiography, including real-time 3-D rendering, simultaneous electrograms and RF ablation procedures.

METHODS

Volumetric scanner system

We used a commercial US scanner capable of generating a real-time 3-D pyramidal scan (Volumetrics Medical Imaging, Durham, NC). The system has 256 receivers and up to 512 variable pulse transmitters. The scanner uses 16:1 parallel receive processing and generates 4100 B-mode lines at up to 30 volumes per s. As shown in Fig. 1, we can display simultaneous orthogonal B-scans, C-scans or inclined planes, all in real-time. By integrating and spatially filtering between two user-selected planes, the system also displays real-time 3-D rendered images. The entire volume of image data is projected onto a 2-D plane by using "ray casting" techniques to project a 2-D array of rays through the 3-D scan data (Fenster and Downey 1996).

Transducer fabrication

The transducers used in this study all consist of a 13 × 11 array including 64 active channels operating at 5 MHz in a 12 French catheter lumen (o.d. = 3.8 mm). We used the Field program by Jensen (Jensen and Svendsen 1992) to simulate and aid the design of our 2-D array. Figure 2 shows the simulated results of our transducers, including angular beam plot (Fig. 2a) and the −6-dB and −20-dB beam-widths plotted as a function of depth (Fig. 2b). As can be seen in Fig. 2b, based on the −6-dB beam-width, our transducers should be able to image a 4-mm lumen out to a depth of approximately 3 cm. This is demonstrated in Fig. 3 where a 4-mm hole in a sponge phantom is seen in both the B-scan and real-time C-scan.

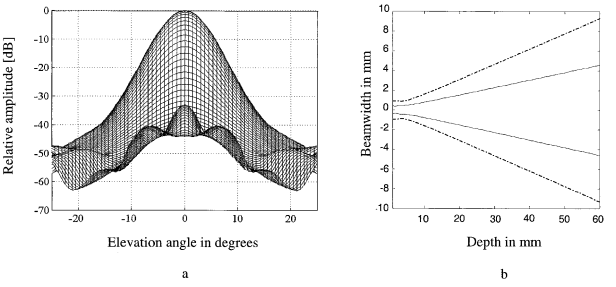

Fig. 2. Simulated beam-widths of the transducer. (a) The beam-width at 30 mm. (b) The −6 and −20-dB contours of the beam-width vs. depth out to 60 mm. The dashed line is the −20-dB contour.

All transducers were constructed on a multilayer flex circuit as previously described (Fiering et al. 2000; Light el al. 1998). Figure 4 shows a photograph of the multilayer polyimide flexible (Fig. 4a) circuit and a completed 2-D array (Fig. 4b).

There are two configurations for the transducers, side-scanning and beveled with respect to the long axis of the catheter lumen. Figure 5 shows a schematic of these two configurations, along with a tip ECG electrode and five ring electrodes added to acquire electrocardiogram signals simultaneously.

Animal model

This study was approved by the Institutional Animal Care and Use Committee at Duke University and conformed to the Research Animal Use Guidelines of the American Heart Association. Three domestic sheep were used for the *in vivo* images shown in this paper. The hearts for the *in vitro* images were obtained from two other domestic sheep.

The sheep were sedated with ketamine hydrochloride 15 to 22 mg/kg IM, and an IV line established in a peripheral vein. Anesthesia was maintained with isoflu-

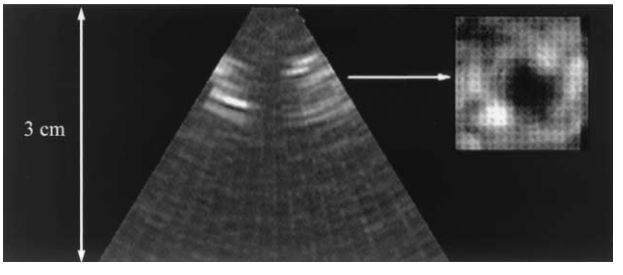

Fig. 3. An image of a 4-mm hole in a sponge, showing a B-scan and real-time C-scan. The arrow indicates the plane of the C-scan within the pyramidal volume.

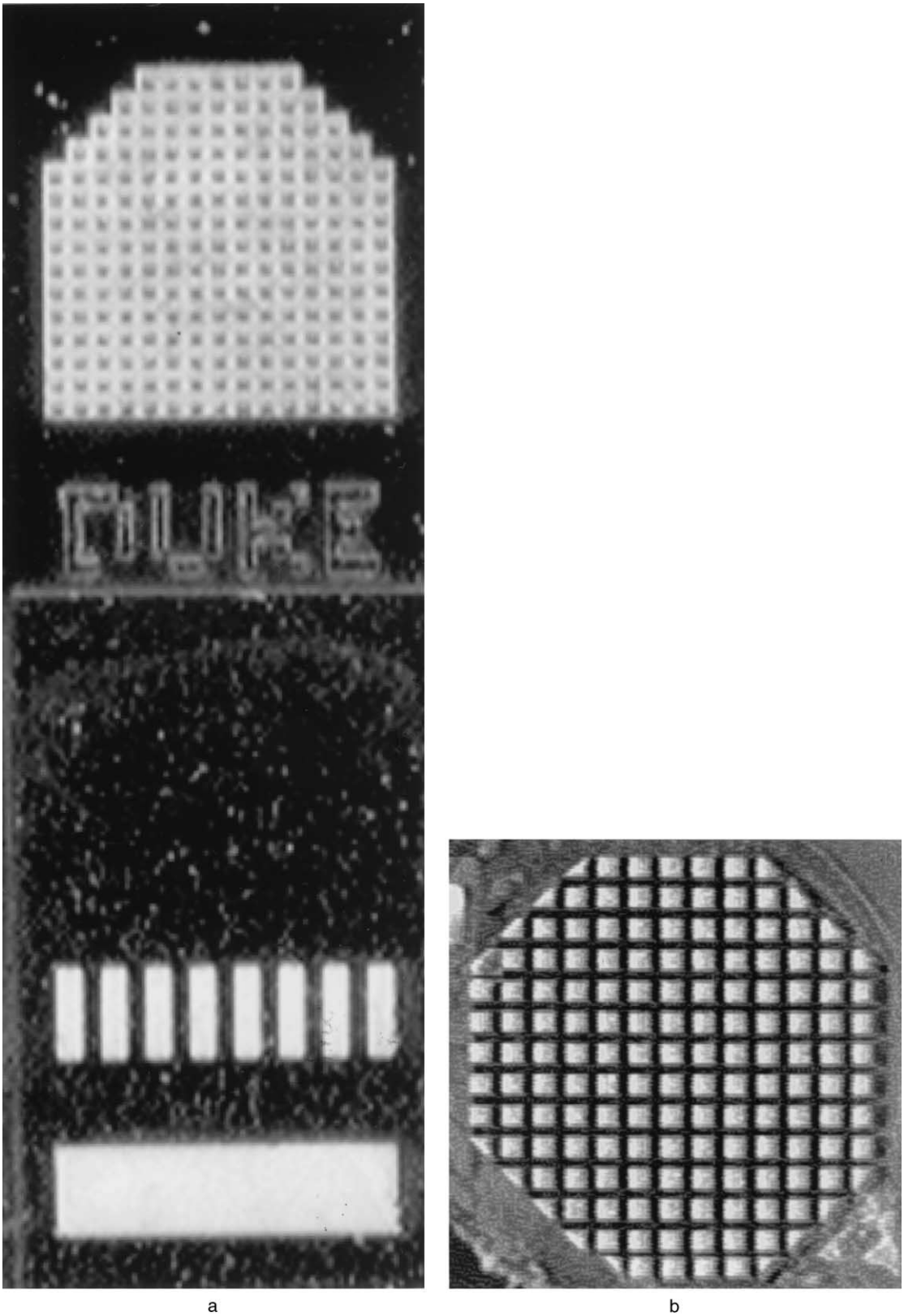

a b

Fig. 4. (a) Closeup of the multilayer flex used to fabricate our transducer. The pads on the top of the image connect to the PZT. The first row of eight solder pads and their common ground pad can be seen in the bottom of the image. (b) The diced array. The inter-element spacing is 0.2 mm, with a 0.025-mm saw kerf, the individual elements are 0.175 mm on a side.

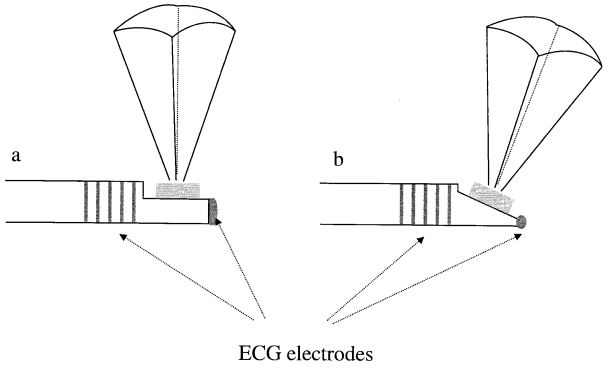

Fig. 5. Schematic showing the two transducer orientations. (a) Side-scanning and (b) beveled with the five ring electrodes and the tip electrode on each.

rane gas 1% to 5% delivered through a nose cone. The animals were placed on their backs on a water-heated thermal pad and a tracheotomy was performed to place an endotracheal tube. The animals were placed on their left sides and started on a respirator (North American Drager; Telford, PA). To prevent rumenal typany, a nasogastric tube was passed into the stomach. A femoral arterial line was placed on the left side *via* a percutaneous puncture. Electrolyte and respirator adjustments were made, based on serial electrolyte and arterial blood gas measurements. An IV maintenance fluid with 0.9% sodium chloride was maintained at 5 mL/kg/min. Blood pressure, lead II electrocardiogram and temperature were continuously monitored throughout the procedure.

Intracardiac echocardiography

Our prototype transducers were not fitted with mechanical steering mechanisms. To overcome this limitation, all the *in vivo* images were acquired after median sternotomy to expose the heart. Small incisions were made in the appropriate cardiac chambers to allow access for our imaging catheter. The incisions were then closed with a purse-string suture.

For the *in vitro* imaging of the pulmonary veins, the veins were removed along with part of the left atrium from the sheep heart and placed in a water bath. For the ablation study, a freshly excised piece of interventricular septum was placed in a small water bath for imaging purposes. An ablation catheter (Cardiac Pathways, model 8002, radii T) was used to create a septal lesion by heating the tip to 70°C for 1 min.

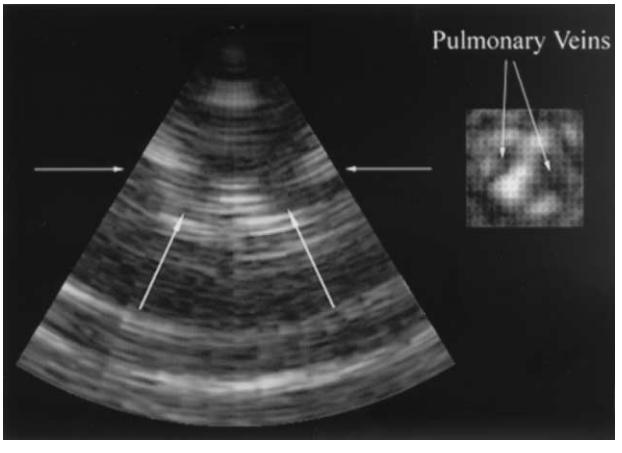

Fig. 6. An image of the pulmonary veins *in vitro*. The arrows next to the B-scan indicate the plane of the simultaneous C-scan. The pulmonary veins are indicated in both the B-scan and the C-scan.

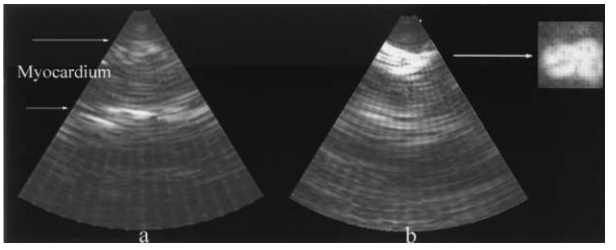

Fig. 7. The results from an *in vitro* ablation study. B-scans of the tissue in a water tank (a) before being ablated and (b) after ablation with the corresponding C-scan. The arrows in (a) indicate the anterior and posterior walls of the excised septum in the image. The maximum depth of the lesion as measured by the scanner in the B-scan is 0.4 cm. The arrow in (b) indicates the plane of the C-scan in the pyramidal volume.

RESULTS

In vitro

Figure 6 shows the results of *in vitro* imaging of the pulmonary veins. The B-scan shows the long axis of the two veins, and the os of the two veins in an *en face* view can be seen in the real-time C-scan. Using the scanner computation package, we measured the cross-sectional

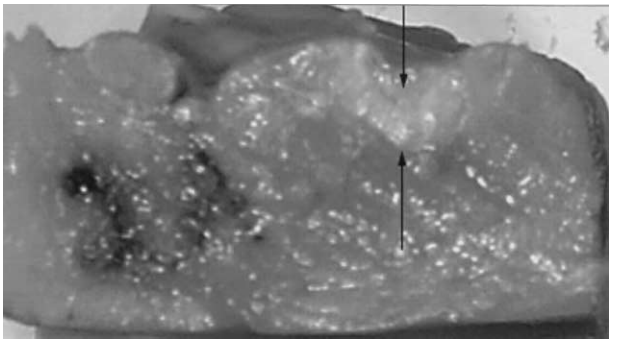

Fig. 8. The histology of the lesion shown in Fig. 7. The lesion area is indicated by the arrows and was measured to be 0.34 cm deep.

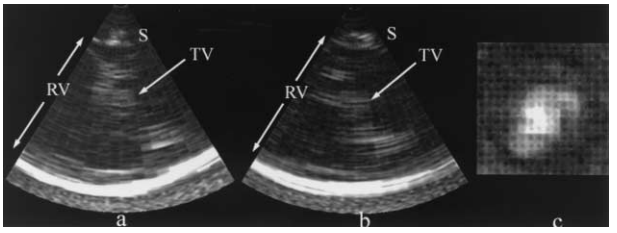

Fig. 9. The RV, as imaged from the LV, showing the interventricular septum (S) and a portion of the tricuspid valve (TV). (a), (b) Two orthogonal B-scans and (c) the real-time C-scan of a portion of the TV.

area of the two pulmonary veins and calculated diameters of 3 and 6 mm, respectively.

Figure 7 shows the results from our ablation study. The tissue is located 1 cm from the face of the transducer and is approximately 2 cm thick. Figure 7a is a B-scan control image before the ablation, and Fig. 7b shows the same B-scan after the ablation procedure with a real-time C-scan through the lesion. The created lesion is clearly more echogenic than the surrounding tissue. Figure 8 shows the histologic slice of the lesion. Using the US system, the maximum depth of the lesion was measured to be 0.40 cm. Histology showed a maximum depth of 0.34 cm.

In vivo

From within the left ventricle. After an apical puncture, the catheter array was inserted into the left ventricle (LV) and oriented to scan across the ventricular septum into the right ventricle. Figure 9 shows images of the right ventricle (RV) taken from the left ventricle. The interventricular septum is seen, as well as the right ventricle. Portions of the tricuspid valve can also be seen in both the orthogonal B-scan views (Fig. 9a and b). Figure 9c shows an *en face* view of the valve leaflet in the real-time C-scan.

Figure 10a shows another view from the LV. Again, we see the interventricular septum, as well as the RV. We also simultaneously acquired three bipolar intracavity electrogram signals from the LV wall. Figure 10b shows the signals compared to the external ECG lead III. The catheter signals all line up with the QRS complex of the external lead. This confirms the location of the catheter electrodes within the left ventricle because the QRS complex is an indicator of LV electrical polarization.

From within the left atrium. The catheter array transducer was then moved up through the mitral valve from the LV into the left atrium (LA). Figure 11a shows an image of the left atrium and the right atrium (RA) acquired from the left atrium. Figure 11b shows three

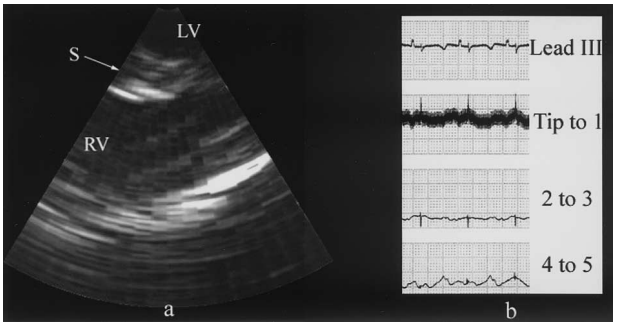

Fig. 10. (a) The RV from the LV, showing the interventricular septum (S) with (b) three simultaneous bipolar electrocardiograms. Note that the ECG signals line up with the QRS complex of the external ECG.

bipolar ECG signals compared to the external lead III. The signals from the first two pairs line up with the P wave, an indicator of LA polarization. However, the last signal lines up with the QRS complex, an indicator of LV polarization. The first two electrode pairs are in the LA, whereas the last pair of electrodes (most proximal) is still in the LV.

Figure 12 shows a four-chamber view obtained from the LA. In this case, a small incision was made in the LA and our transducer inserted. The interatrial septum is clearly seen in the B-scan (Fig. 12a). The two C-scans (Fig. 12b and c) show the *en face* view of the mitral valve open (Fig. 12b) and closed (Fig. 12c).

From within the right ventricular outflow tract. Figure 13 shows an image of the pulmonic valve from the RV outflow tract. The valve is closed in the B-scan (Fig. 13a). In the real-time 3-D rendered views, the valve is open in Fig. 13b and closed in Fig. 13c, where we can see the three leaflets.

From the right atrium. Figure 14 shows the tricuspid valve as imaged from the RA. We see the valve

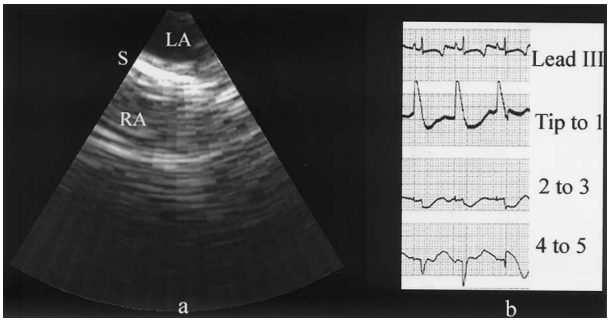

Fig. 11. (a) B-scan of the LA and RA from within the LA, showing the interatrial septum (S), with (b) simultaneous bipolar electrocardiogram. Note that the first two (tip to 1 and 2 to 3) ECG signals line up with the P-wave and the last (4 to 5) signal lines up with the QRS complex of the external ECG.

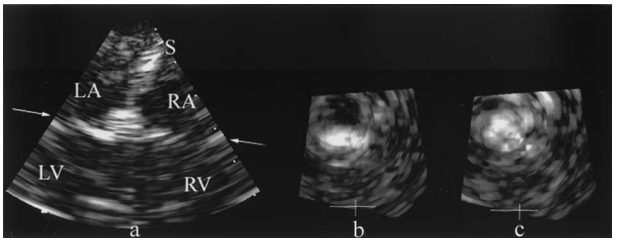

Fig. 12. Four-chamber view of a sheep heart from the LA. (a) Note the interatrial septum (S), RA, LV and RV in the B-scan. The arrows in the B-scan indicate the inclined plane of the C-scans. The mitral valve can be seen (b) open and (c) closed in the two C-scans.

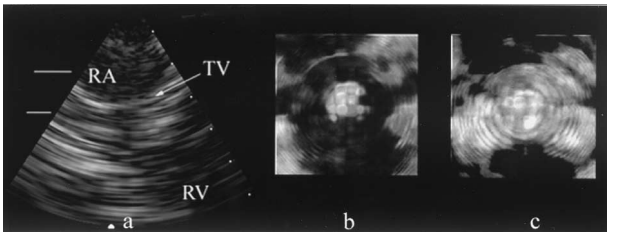

Fig. 14. (a) The tricuspid valve, as imaged from the RA looking into the RV. The B-scan of the valve (TV) shows it closed. The lines to the left of the B-scan indicate the planes that are the boundaries of the rendered volume. The real-time 3-D rendered views show it (b) open and (c) closed. There is an electronic noise artefact in (b).

closed in the B-scan (Fig. 14a). In the two real-time 3-D rendered views, the valve is shown open (Fig. 14b) and closed (Fig. 14c). In the volume-rendered view of the closed valve, we can clearly see the three leaflets *en face*.

Figure 15 shows an image of two interventional devices inside the RA, an atrial pacing lead and an electrophysiological mapping catheter. The B-scan (Fig. 15a) shows a cross-section of the pacing lead and a long axis view of a quadripolar mapping catheter. The real-time volume-rendered view (Fig. 15b) gives more detail of their spatial orientations, showing the devices crossing within the atrium.

DISCUSSION

We have shown real-time volumetric intracardiac images using a 2-D catheter array transducer. We have imaged major anatomical landmarks *in vivo*, such as the mitral valve, tricuspid valve, interatrial septum and the RV. Also, we were able to image other interventional devices within the heart with an improved perspective view, using the real-time volume rendering feature. Thus, real-time 3-D intracardiac echocardiography may become a valuable tool in guiding interventional cardiac procedures.

We also monitored and quantified an RF ablation study *in vitro*. The lesion showed high contrast compared to normal myocardium in the US image.

Finally, we have shown that a US imaging transducer can be combined with an EP mapping device. This could lead to a single combined device that will image the heart, find areas of arrhythmia with the mapping electrodes, deliver the RF ablation and, again, image the heart to view and quantify the lesion.

Device limitation and need for improvement

The primary limitation of our current catheter transducers is the lack of mechanical steering. A fully steerable catheter array would allow us to obtain equivalent images in closed-chest subjects. In addition, the current 12-French catheter transducers are too large for routine clinical use. We are actively pursuing the development of transducer arrays in a 9-French catheter and have recently shown prototype devices with up to 70 channels in a 9-French device (Fiering et al. 2000).

To improve image quality, we need more transducer channels and improved transducer materials. New cable

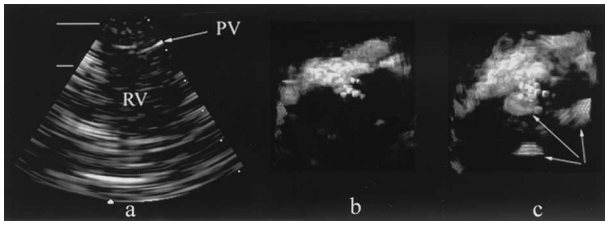

Fig. 13. An image of the pulmonic valve (PV) from the RV outflow track. (a), (c) The valve closed, and (b) open. (b), (c) Real-time 3-D rendered views created between the planes shown to the left of the B-scan in (a). The arrows in (c) indicate the three leaflets of the valve.

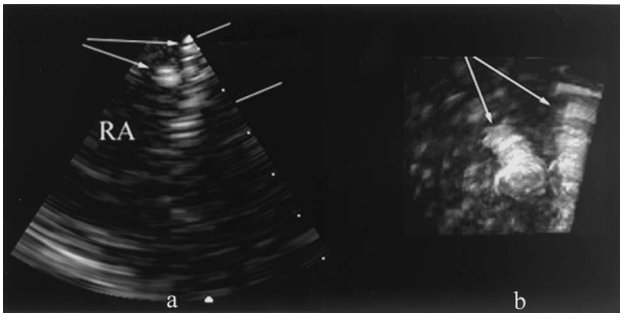

Fig. 15. Images of two EP catheters in the RA. The imaging transducer is also placed in the RA. (a) The two catheters (arrows) are seen in the B-scan, but their relative positions are more obvious in (b) the rendered view. The lines in the right of the B-scan indicate the planes that are the boundaries of the rendered volume.

technology and the use of multiplexer switches within the catheter may solve these problems. The use of improved acoustic matching layers, multilayer piezoelectric ceramics or single crystal ferroelectrics can improve the SNR by up to 20 dB (Goldberg and Smith 1994). We are also pursuing higher frequency transducers for improved spatial resolution, where depth of penetration is not a limitation. We have previously developed transthoracic 2-D array transducers operating at up to 10 MHz (Light et al. 1999; Light et al. 2000), and we believe that we can extend this technology to intracardiac 2-D array transducers of frequencies of up to 20 MHz.

REFERENCES

Bom N, Lancee CT, Van Egmond FC. An ultrasonic intracardiac scanner. Ultrasonics 1972;10:772–776.

Fenster A, Downey DB. 3-D ultrasound imaging: A review. IEEE Eng Med Biol Mag 1996;15(6):41–51.

Fiering JO, Hultman PA, Lee W, Light ED, Smith SW. High density interconnect for two dimensional arrays. IEEE Trans Ultrason Ferro Freq Control 2000;47:764–770.

Goldberg RL, Smith SW. Multilayer piezoelectric ceramics for two-dimensional array transducers. IEEE Trans Ultrason Ferro Freq Control 1994;41:761–771.

Jensen JA, Svendsen NB. Calculation of pressure fields from arbitrarily shaped, apodized, and excited ultrasound transducers. IEEE Trans Ultrason Ferro Freq Control 1992;39:262–267.

Light ED, Davidsen RE, Fiering JO, Hruschka TA, Smith SW. Progress in two dimensional arrays for real-time volumetric imaging. Ultrason Imaging 1998;20:235–250.

Light ED, Fiering JO, Hultman PA, Lee W, Smith SW. Update of two dimensional arrays for real-time volumetric and real-time intracardiac imaging. Proc IEEE Trans Ultrason Sympos 1999;H37027: 1217–1220.

Light ED, Hultman PA, Idriss SF, Lee W, Wolf PD, Smith SW. Two dimensional arrays for real-time volumetric and intracardiac imaging with simultaneous electrocardiogram. Proc IEEE Trans Ultrason Sympos 2000;00CH37121:1195–1198.

Qin JX, Jones M, Shiota T, Greenberg NL., et al. Validation of real-time three- dimensional echocardiography for quantifying left ventricular volumes in the presence of a left ventricular aneurysm: In vitro and in vivo studies. J Am Coll Cardiol 2000;36: 900–907.

Ren JF, Schwartzman D, Michele JJ, et al. Lower frequency (5-MHz) intracardiac echocardiography in a large swine model: Imaging views and research applications. Ultrasound Med Biol 1997;23: 871–877.

Schmidt MA, Ohazama CJ, Agyeman KO, et al. Real-time three-dimensional echocardiography for measurement of left ventricular volumes. Am J Cardiol 1999;84:1434–1439.

Seward JB, Packer DL, Chan RC, Curley MC, Tajik AJ. Ultrasound cardioscopy: Embarking on a new journey. Mayo Clin Proc 1996; 71:629–635.

Shiota T, Jones M, Chikada M, et al. Real-time three-dimensional echocardiography for determining right ventricular overload. Circulation 1998;97:1897–1900.

Smith SW, Pavy HE, von Ramm OT. High speed ultrasound volumetric imaging system part I: Transducer design and beam steering. IEEE Trans Ultrason Ferro Freq Control 1991;38:100–108.

Stetten GD, Ota T, Ohazama CJ, et al. Real-time 3D ultrasound: A new look at the heart. J Cardiovasc Diagn Procedures 1998;15:73–84.

Wharton JM, Ideker RE. Cardiac mapping of supraventricular and ventricular arrhythmias in the electrophysiology laboratory and operating room. In: Podrid PJ, Kowey PR, eds. Cardiac arrhythmia: Diagnosis and management. Baltimore: Williams and Wilkins, 1995:323–346.